Catal Lett (2012) 142:1067–1074
DOI 10.1007/s10562-012-0864-7

Superior Performance of Mesoporous TiO_2–Al_2O_3 Supported NSR Catalysts with the Support Synthesized Using Nonionic and Cationic Surfactants as Co-Templates

Zhongbo Li · Ming Meng · Rui You · Tong Ding · Zhijun Li

Received: 12 April 2012 / Accepted: 25 June 2012 / Published online: 12 July 2012

Abstract Mesoporous binary oxides TiO_2–Al_2O_3 were prepared by citric acid complexation-organic template decomposition method using nonionic *p*-octyl polyethylene glycol phenyl ether (OP) and cationic cetyltrimethylammonium bromide (CTAB) as co-templates; the corresponding NSR catalysts Pt/K/TiO_2–Al_2O_3 were prepared by successive wetness impregnation. Multiple techniques including N_2 physisorption, XRD, HR-TEM, NH_3-TPD, H_2-TPR and H_2-chemisorption were employed for catalyst characterization. It is found that the support prepared using OP and CTAB as co-templates possesses much larger specific surface area (309 m^2/g) than those prepared using CTAB as single template (275 m^2/g) or using conventional co-precipitation (250 m^2/g); meanwhile, this support exhibits the largest amount of surface acidic sites as indicated by NH_3-TPD results, which makes its supported catalyst show the best sulfur-resistance performance among the catalysts with the support prepared by different methods. The results of H_2-chemisorption and HR-TEM conformably indicate that this catalyst also possesses the highest dispersion of Pt, which determines its best NOx storage and reduction performance at lean/rich cycles, giving a mean NOx reduction percentage as high as 95 %.

Keywords Co-templates · NOx storage and reduction · Sulfur resistance · Mesoporous TiO_2–Al_2O_3

Z. Li · M. Meng (✉) · R. You · T. Ding
Tianjin Key Laboratory of Catalysis Science and Engineering, School of Chemical Engineering and Technology, Tianjin University, Tianjin 300072, People's Republic of China
e-mail: mengm@tju.edu.cn

Z. Li
State Key Laboratory of Engines, Tianjin University, Tianjin 300072, People's Republic of China

1 Introduction

To save the limited fossil fuels, lean-burn technique should be developed and widely applied to engines. However, a bottle-neck namely the formation of nitrogen oxides (NOx) at lean-burn condition has hindered the extensive application of this technique, because the as-formed lean-burn NOx species cannot be effectively removed by traditional three-way catalysts (TWC) [1]. So, developing new techniques or new catalysts to eliminate the lean-burn NOx is urgently necessary. At present, the most promising approach for its removal is the NOx storage-reduction (NSR) technique [2], which can trap the NOx species during lean-burn period, and reduce these species to N_2 at rich condition [3].

Up to now, the most popular and classical NSR catalyst is Pt/Ba/Al_2O_3, which has been industrialized in Japanese market where no sulfur or ultra-low content of sulfur is contained in the fuels. However, in most markets of the world, the fuels contain some sulfur species which can cause the permanent deactivation of NSR catalysts by the formation of highly thermo-stable barium sulfates [4–7]. Our previous work and the research of other groups have shown that using K as storage material and acidic oxides as supports (e.g., TiO_2–Al_2O_3, TiO_2–ZrO_2–Al_2O_3) can increase both the NOx storage capacity (NSC) and the sulfur-resistance performance of the NSR catalysts [8–10]. It is well known that the regeneration ability of the sulfated NSR catalysts mainly depends on the kinds of the sulfates and their crystallite size. The small crystallites of sulfates are relatively easier to reduce, however, large crystallites or bulk sulfates are very difficult to reduce. So, the dispersion of storage component in NSR catalysts is rather important. To ensure the high dispersion of storage component and the high regeneration ability of NSR catalysts, the supports

should possess as large as specific surface area. In addition, the large specific surface area of the supports is also favorable to the dispersion of noble metals, which can enhance the performance of the NSR catalysts for NO oxidation, NOx storage at lean condition and reduction at rich condition.

In the last two decades, many kinds of mesoporous materials such as SBA-15 and MCM-41 Si-based materials, etc. [11, 12] have been successfully synthesized, which exhibit very large specific surface area. To acquire large specific surface area and high component dispersion for the NSR catalysts, in this work, the method of preparing mesoporous Si-containing molecular sieves was used for reference to prepare the mesoporous TiO_2–Al_2O_3 binary oxide supports by using the nonionic *p*-octyl polyethylene glycol phenyl ether (OP) and the cationic cetyltrimethylammonium bromide (CTAB) as co-templates. The NOx storage/reduction performance and the sulfur-resisting ability of the corresponding Pt/K/TiO_2–Al_2O_3 catalyst are much better than those using the supports obtained by conventional co-precipitation method or by using CTAB as single template.

2 Experimental

2.1 Support and Catalyst Preparation

2.1.1 Support Preparation using CTAB as Single Template

Firstly, according to the optimized weight ratio of TiO_2/(TiO_2 + Al_2O_3) = 0.4 (molar ratio: Ti/Ti + Al = 0.3) in our previous study [9], given amounts of $AlCl_3{\cdot}6H_2O$ and $TiCl_4$ were dissolved in deionized water to form a solution, then the citric acid with a molar amount of 1.1 times of all the cations was added to this solution to ensure the complete complexation of all the metal ions. In the next, given amount of CTAB with a molar ratio of CTAB/(Ti + Al) = 0.3 was added to the above solution. After continuous stirring for 30 min, ammonia was dropwise added to adjust the pH value to 9 ± 0.5. The resulting slurry was stirred for 3 h at room temperature, then transferred to a Teflon autoclave, which was sealed and kept at 120 °C for 12 h to increase the degree of condensation. After filtration and washing with ethanol, the solid product was dried overnight in air at 120 °C, and finally calcined in air at 550 °C for 6 h to thoroughly remove the organic template. The obtained support is denoted as TA-CTAB, where TA stands for TiO_2–Al_2O_3 binary oxides.

Support preparation using OP and CTAB as co-templates: the preparation procedure for this support is almost the same as that for TA-CTAB, only the template CTAB was replaced by the mixture of OP and CTAB (molar ratio: OP/CTAB = 0.4), but the whole molar amount of the mixed templates is unchanged. The as-synthesized support is denoted as TA-CTAB-OP.

Support preparation by conventional co-precipitation: for comparison, the support was also prepared by co-precipitation using ammonia as precipitate reagent. The procedure is also similar to that for TA-CTAB preparation, but no any citric acid and templates were added to the solution containing Ti or Al ions before precipitation. The support synthesized by this method is denoted as TA-CO.

2.1.2 Catalyst Preparation

The NOx storage and reduction catalysts Pt/K/TiO_2–Al_2O_3 (Pt: 1 wt%; K: 5 wt%) were prepared by sequential impregnation. Briefly, an aqueous solution of $H_2PtCl_6{\cdot}6H_2O$ was firstly impregnated into the pores of the synthesized TA supports, then dried at 120 °C overnight and calcined at 550 °C for 3 h in air to get Pt/TiO_2–Al_2O_3 precursor. This precursor was subsequently impregnated into an aqueous solution of KNO_3. After drying and calcination under the same condition above, the target catalysts were obtained, which are denoted as Pt/K/TA-CTAB, Pt/K/TA-CTAB-OP and Pt/K/TA-CO, respectively.

2.2 Catalyst Pretreatment

Before use, each catalyst (400 mg) was pretreated in pure H_2 at 350 °C for 60 min in a quartz-tubular continuous flow reactor (i.d. = 8 mm and L = 600 mm) with a flow rate of 150 mL/min. To evaluate the desulfation/regeneration behavior of the catalysts, the freshly reduced catalysts was pretreated at 350 °C for 90 min in the atmosphere containing 100 ppm SO_2, 5 vol% O_2 and balance N_2 (150 mL/min) to get sulfated samples, which will be used for H_2-TPR measurement to investigate the desulfation performance of the catalysts; meanwhile, part of the sulfated catalysts was regenerated by H_2 reduction at the same condition as above, and used for NOx storage experiment to investigate the regeneration efficiency.

2.3 Catalyst Characterization

The specific surface area (S_{BET}) of the samples was measured at −196 °C on a Quantachrome QuadraSorb SI instrument by using the nitrogen physi-sorption method. The samples were pretreated in vacuum at 300 °C for 8 h before experiments. The S_{BET} was determined from the linear part of the BET curve. The pore diameter distribution was calculated based on the desorption branch using the BJH formula.

X-ray diffraction measurement was carried out on an X'pert Pro rotatory diffractometer (PANAlytical) operating

at 40 mA and 40 kV using Cu Kα as radiation source ($\lambda = 0.15418$ nm). The data of 2θ from 20 to 90° was collected with the step size of 0.033°.

NH_3-TPD measurement was conducted in a conventional flow apparatus equipped with a thermal conductivity detector. 300 mg supports were first pretreated at 500 °C for 0.5 h under pure helium with a flow rate of 30 mL/min, then exposed to a gas mixture flow of 10 % vol NH_3 + 90 % vol N_2 at 100 °C for half an hour. Thereafter, the sample was purged by helium with a flow rate of 30 mL/min at the same temperature until the baseline is stable. In the next, the sample was heated to 550 °C at a rate of 5 °C/min to get the TPD profile.

Temperature-programmed reduction (TPR) was performed on a TPDRO 1100 apparatus supplied by Thermo-Finnigan Company. Before detection by the TCD, the gas was purified by a trap containing CaO + NaOH materials in order to remove the H_2O and CO_2. Each time, 30 mg of the sample were heated from room temperature to 900 °C at a rate of 10 °C/min. A gaseous mixture of 8 vol% H_2 in N_2 was used as reductant at a flow rate of 30 mL/min.

The Pt dispersion was estimated on the freshly reduced catalysts by (i) hydrogen chemisorption using the above TPDRO instrument at 25 °C and (ii) HR-TEM measurements using a side-entry Jeol JEM 2100F (200 kV) microscope.

2.4 Measurement of NSC and Reduction Percentage in Lean/Rich Cycles

NSC measurements for both the fresh and sulfur-aged catalysts were carried out in the quartz-tubular continuous flow reactor (i.d. 8 mm) loaded with 400 mg catalyst (40–60 mesh) at lean condition. Each time, the sample was first heated to 350 °C, then a mixture gas containing 400 ppm NO, 5 vol% O_2 and balance N_2 was introduced to the reactor at a rate of 400 mL/min. The concentrations of NO, NO_2 and total NOx at the reactor outlet were continuously monitored by an online Chemiluminescence NO–NO_2–NOx Analyzer (Model 42*i*-HL, Thermo Scientific) until the outlet concentration of total NOx reached the level of inlet and kept constant. NSC was calculated by integrating the concentration curves of NOx.

The performance of the sample for NOx reduction was evaluated in lean/rich cycles. The experiments were conducted in the same reactor as for the NSC measurement with a lean period of 7 min and a rich period of 1 min. In lean period the mixture gas of 400 ppm NO + 5 vol% O_2 + balance N_2 was introduced to the sample with a flow rate of 400 mL/min, while in rich period the oxygen was replaced by 1,000 ppm C_3H_6. In each case, enough cycles were performed so that the data presented can reflect the average level; the mean NOx reduction percentage was calculated by integrating the concentration curves of NOx based on the last two cycles, in which the catalysts have shown relatively stable performance.

3 Results and Discussion

3.1 Structural Properties

The nitrogen adsorption/desorption isotherm of the catalyst TA-CTAB (not shown) exhibits type IV shape, and its BJH pore size distribution is centered at ca. 3.85 nm. From the linear part of the isotherms, the specific surface area of TA-CTAB was calculated, which is 275 m^2/g. The sample prepared using CTAB and OP as co-templates (TA-CTAB-OP) also possesses type IV isotherm and exhibits mesoporous pore size distribution, however, the BJH pore size distribution is centered at higher position of ca. 5.99 nm. Meanwhile, the BET specific surface area of this sample is increased to 309 m^2/g. For comparison, the BET specific surface area of the sample prepared by co-precipitation is also measured. Table 1 lists all the texture data of the supports and catalysts. It is obvious that the specific surface area of the supports prepared by different methods shows the following order: TA-CTAB-OP > TA-CTAB > TA-CO. After the deposition of Pt and K, the specific surface area of all the supports decreases to some extent due to the partial blocking of pores by the supported components, while the order is unchanged. Here, it should be indicated that since the support TA prepared by using OP alone possesses much lower specific surface area (193 m^2/g) than TA-CTAB-OP, TA-CTAB and TA-CO, its supported catalyst was not prepared and investigated further. In a summary, for the synthesis of mesoporous TiO_2–Al_2O_3 support the method using CTAB and OP as co-templates does show obvious advantages, as compared with those using CTAB as single template or using conventional co-precipitation method.

The effect of the co-templates on the specific surface area and pore diameter of the support TiO_2–Al_2O_3 could be explained by the surfactant packing parameter, $g = V/(a_0L)$, where V is the total volume of the surfactant chains, a_0 is the effective head group area at the organic–inorganic interface and L is the kinetic surfactant chain length [13, 14]. It is known that the polar part of the nonionic surfactant OP is a polymer—$(EO)_n$ with big volume; when it is tied in the micelle formed by CTAB, the curvature of the polar part of the micelle will be remarkably reduced, resulting in the decline of the value of a_0. Furthermore, the hydrophobic part of OP has not only an alkyl chain but also a phenyl ring with a π electron, which has stronger dispersive ability than alkyl chains. The hydrophobic part of OP may embed in the interspace of the micelle formed by CTAB, interacting with the hydrophobic alkyl chains of the

Table 1 Texture data of the supports and catalysts, the dispersion and particle size of Pt in the NSR catalysts

Sample	S_{BET} (m^2/g)	Pore volume (cm^3/g)	Pt dispersion (%)	Particle size of Pt (nm)[a]
TA-CO	250	0.536	–	–
TA-CTAB	275	0.475	–	–
TA-CTAB-OP	309	0.585	–	–
Pt/K/TA-CO	168	0.278	27	3.14
Pt/K/TA-CTAB	186	0.381	30	2.83
Pt/K/TA-CTAB-OP	264	0.465	51	1.67

[a] Calculated from the H_2 chemisorption results

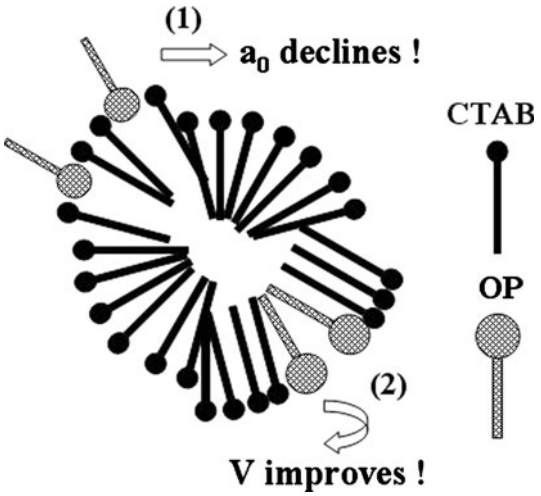

Fig. 1 The effect of the co-templates on the specific surface area and pore diameter of the support TiO_2–Al_2O_3

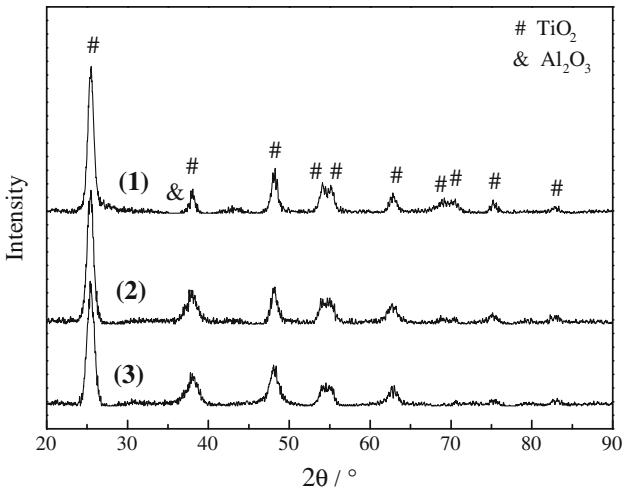

Fig. 2 XRD patterns of the supports prepared by different methods (*1*) TA-CO; (*2*) TA-CTAB; (*3*) TA-CTAB-OP

micelle, as a result, the total volume of the surfactant chains (V) of the micelle is increased [14], as shown in Fig. 1. Both the decrease of a_0 and the increase of V will increase the surfactant packing parameter g, leading to the increase of pore size and specific surface area of the support.

The much larger specific surface area of TA-CTAB-OP should be favorable to the dispersion of noble metal Pt and storage component K. The Pt dispersion and the calculated particle size for the freshly reduced catalysts prepared by different methods was measured by H_2-chemisorption, the results of which are listed in Table 1. It can be seen that the Pt dispersion on the sample synthesized by using co-templates is approximately 51 %, extremely higher than that for other two samples. Meanwhile, the Pt particle size on this sample is only about 1.67 nm, much smaller than that on the other two samples. Generally, Pt plays a key role in both NOx storage and reduction processes [15, 16], so, the higher dispersion of Pt in TA-CTAB-OP should be favorable to the overall performance of this catalyst, as discussed later.

Figure 2 depicts the X-ray diffraction patterns of the supports prepared by different methods. The crystalline anatase TiO_2 (ASTM/PDF 21-1272) is clearly identified, while Al_2O_3 is hard to detect due to the very low intensity or the overlapping of the diffraction peaks, which suggests that the Al_2O_3 exists in amorphous state [9]. By comparison, it is found that the diffraction peaks of the sample synthesized using CTAB and OP as co-templates are wider than those for the samples prepared using CTAB as single template or using co-precipitation method, especially at the high angle region ($2\theta > 65°$), where the diffraction peaks of TiO_2 for TA-CTAB-OP almost disappear. The above results clearly indicate that the crystallites TiO_2 in TA-CTAB-OP are smaller than those in TA-CTAB or TA-CO, which is consistent with the BET results. Since TiO_2 is a kind of solid acidic oxide, the decrease of its crystallite size or increase of its dispersion in TiO_2-based mixed oxide supports could increase the surface acidic sites of the supports, which is extremely beneficial to both the dispersion of basic storage component and the sulfur-resisting ability of the catalysts [10, 17, 18].

The TPD technique using NH_3 as probe molecule was sensitive to the surface acidic sites [19], so, it was employed to evaluate the acidic property of the supports prepared by different methods, the results of which are shown in Fig. 3. From the NH_3-TPD profiles, it can be

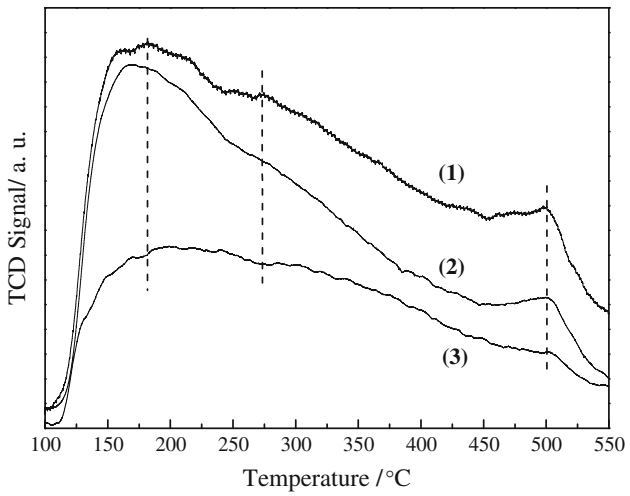

Fig. 3 NH_3-TPD profiles of the supports prepared by different methods (*1*) TA-CTAB-OP; (*2*) TA-CTAB; (*3*) TA-CO

clearly seen that the predominant peaks in the temperature range of 100–550 °C appear at almost the same position for the three samples, which implies the presence of the same kinds of acidic sites in them. However, the acidic amounts in the three samples roughly judged from the total peak areas are obviously different. The sample TA-CTAB-OP obviously possesses much larger amount of surface acidic sites than other two samples, showing an order of TA-CTAB-OP > TA-CTAB > TA-CO, which is totally consistent with that for the specific surface areas. Since the sulfur-resisting ability of TiO_2-containing NSR catalysts mainly depends on its acidity [9, 10, 20], the NH_3-TPD results could be used to predict the superior sulfur-resistance performance of the Pt/K/TiO_2–Al_2O_3 catalyst with the support prepared using CTAB and OP as co-templates.

3.2 NSC and Sulfur-Resistance Performance of the Catalysts

Isothermal experiments of NOx sorption over Pt/K/TiO_2–Al_2O_3 catalysts (both the fresh and the regenerated ones) with the supports prepared by different methods were carried out, and the concentration curves of outlet NOx as a function of time are presented in Figs. 4 and 5. The NSC of all the fresh and regenerated catalysts, as well as the recovery efficiency are listed in Table 2. From Fig. 4 and Table 2, it is found that among the three fresh samples the TA-CTAB-OP shows the highest NSC of 407 μmol/g; after sulfation and regeneration, this sample still possesses the highest NSC (see Fig. 5; Table 2), showing the highest recovery efficiency of NSC (94 %). This result is in good agreement with the results of BET, XRD and NH_3-TPD. In a summary, the NSR catalyst Pt/K/TiO_2–Al_2O_3 with the support prepared using CTAB and OP as co-templates

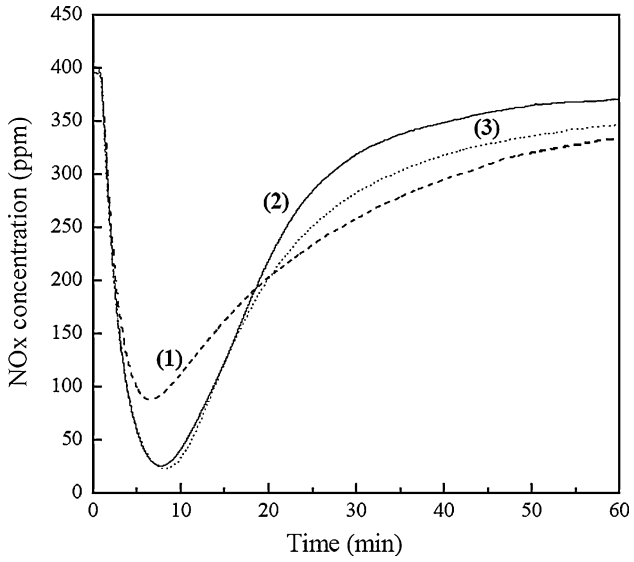

Fig. 4 NOx storage curves of the fresh catalysts Pt/K/TA-CO; (*1*) Pt/K/TA-CO (*2*) Pt/K/TA-CTAB; (*3*) Pt/K/TA-CTAB-OP

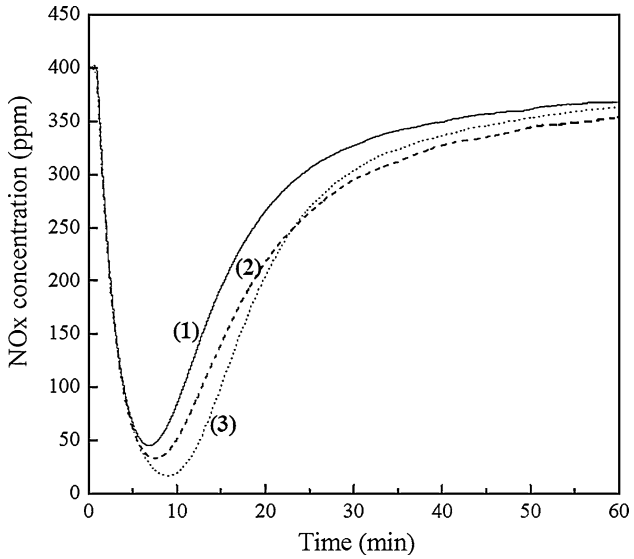

Fig. 5 NOx storage curves of the regenerated catalysts (*1*) Pt/K/TA-CO; (*2*) Pt/K/TA-CTAB; (*3*) Pt/K/TA-CTAB-OP

Table 2 NOx storage capacity (NSC) of the fresh catalysts and sulfated ones after regeneration in 60 min at 350 °C

Sample	NSC (μmol/g)		RE (%)
	Fresh	Regenerated	
Pt/K/TA-CO	364	308	84
Pt/K/TA-CTAB	393	365	92
Pt/K/TA-CTAB-OP	407	382	94

RE: Recovery efficiency is the ratio of the NSC for the regenerated catalyst to that for the corresponding fresh one

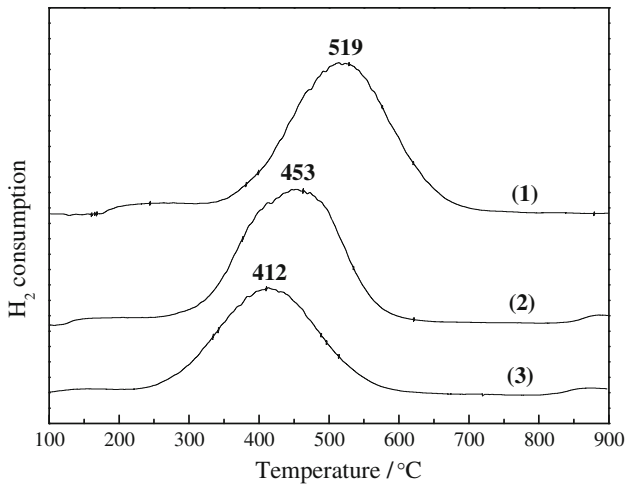

Fig. 6 H_2-TPR profiles of the sulfur-aged catalysts (*1*) Pt/K/TA-CO; (*2*) Pt/K/TA-CTAB; (*3*) Pt/K/TA-CTAB-OP

possesses much better performance in both NOx storage and sulfur resistance as compared with the two catalysts with the support prepared by other methods.

3.3 Desulfation

For clarifying the regeneration behaviors (desulfation) for the sulfated samples, H_2-TPR tests were performed and the profiles are presented in Fig. 6. It can be seen that the H_2 consumption peak for the sulfur-aged catalyst Pt/K/TA-CTAB-OP appears at ca. 412 °C, much lower than those for Pt/K/TA-CTAB (~453 °C) and Pt/K/TA-CO (~519 °C), suggesting the much best desulfation performance of this catalyst. The reduction peaks could be mainly attributed to the reduction of potassium sulfates. Based on the peak areas, the relative ratio of the amounts of potassium sulfates in the three samples is calculated, which is Pt/K/TA-CTAB-OP:Pt/K/TA-CTAB:Pt/K/TA-CO = 1.0:1.1:1.3. If all the sulfur species in sulfated samples were desorbed during H_2-TPR, it can be deduced that less sulfur species has deposited on the catalyst Pt/K/TA-CTAB-OP than on the others. However, the sulfur may also transform to metal sulfides during reduction such as K_2S species, which cannot be desorbed. We ever tried to measure the metal sulfides on the reduced samples by XPS, but no metal sulfides were detected. Combined with the results of BET, XRD and NH_3-TPD, it is concluded that the increased acidic property of the support TA-CTAB-OP should play a key role in the improvement of sulfur-resistance of its supported catalyst, and that larger specific surface area of this support facilitates the dispersion of the basic storage component, thus decreasing the size of as-formed potassium sulfates during sulfation. Generally, the smaller sulfates possess better reducibility. The lowest reduction temperature for the sulfated Pt/K/TA-CTAB-OP suggests that this sample possesses the smallest particle size of sulfates.

3.4 NOx Reduction at Lean/Rich Cycling Conditions

To investigate the performance of the catalysts, the NOx was stored and reduced at lean/rich cycling condition. Figure 7a, b, c show the curves of NOx concentration in reactor outlet at lean/rich cycling condition (8 cycles) over the catalysts Pt/K/TiO_2–Al_2O_3 with the supports prepared by different methods. By comparison of the curves in Fig. 7a, b, c, it is found that during the lean condition the NOx storage behavior of the catalysts Pt/K/TA-CO, Pt/K/TA-CTAB and Pt/K/TA-CTAB-OP is somewhat different. As displayed in Fig. 7a, the NOx concentration gradually increases over Pt/K/TA-CO with the lean time increasing since the storage sites are gradually saturated [21]; at the end of lean period (7 min) for the last several cycles, the NOx concentration reaches ca. 95 ppm (see the dash line). For the sample Pt/K/TA-CTAB, the corresponding NOx concentration is obviously decreased but still more than 40 ppm, as shown in Fig. 7b. However, for Pt/K/TA-CTAB-OP nearly no NOx is detected during the whole lean period even after eight cycles, which further confirms that the catalyst Pt/K/TA-CTAB-OP possesses much better NOx storage performance than the other two. In addition, from Fig. 7, it can still be seen that at the switch moment from lean to rich condition, the NOx concentration suddenly increases. Since the stored nitrate/nitrite species are thermodynamically unstable at rich condition, the rapid increase of NOx concentration may be resulted from the instantaneous decomposition of them. In addition, at the moment from lean to rich condition, the lack of reductant downstream leads to the released NOx from nitrate/nitrite decomposition not effectively reduced, thus increasing the NOx concentration. After the switch moment, the released NOx could be rapidly and effectively reduced by the reductant C_3H_6, making the NOx concentration decrease to a very low level (<10 ppm). According to literature [21–24], the height of NOx peak at the moment from lean to rich condition can reflect the performance of NSR catalysts for NOx reduction, so, it is deduced that the catalyst Pt/K/TA-CTAB-OP also possesses much better NOx reduction performance than the other two. Since the catalysts have shown relatively stable performance at the last two lean/rich cycles, the average NOx reduction percentages over them are calculated based on these two cycles. For Pt/K/TA-CTAB-OP the NOx reduction percentage is as high as 94.8 %, obviously larger than that over the samples Pt/K/TA-CTAB and Pt/K/TA-CO (90.8 and 84.6 %, respectively). The much better performance for NOx storage and reduction of this catalyst should be mainly attributed to the higher dispersion of Pt and storage component.

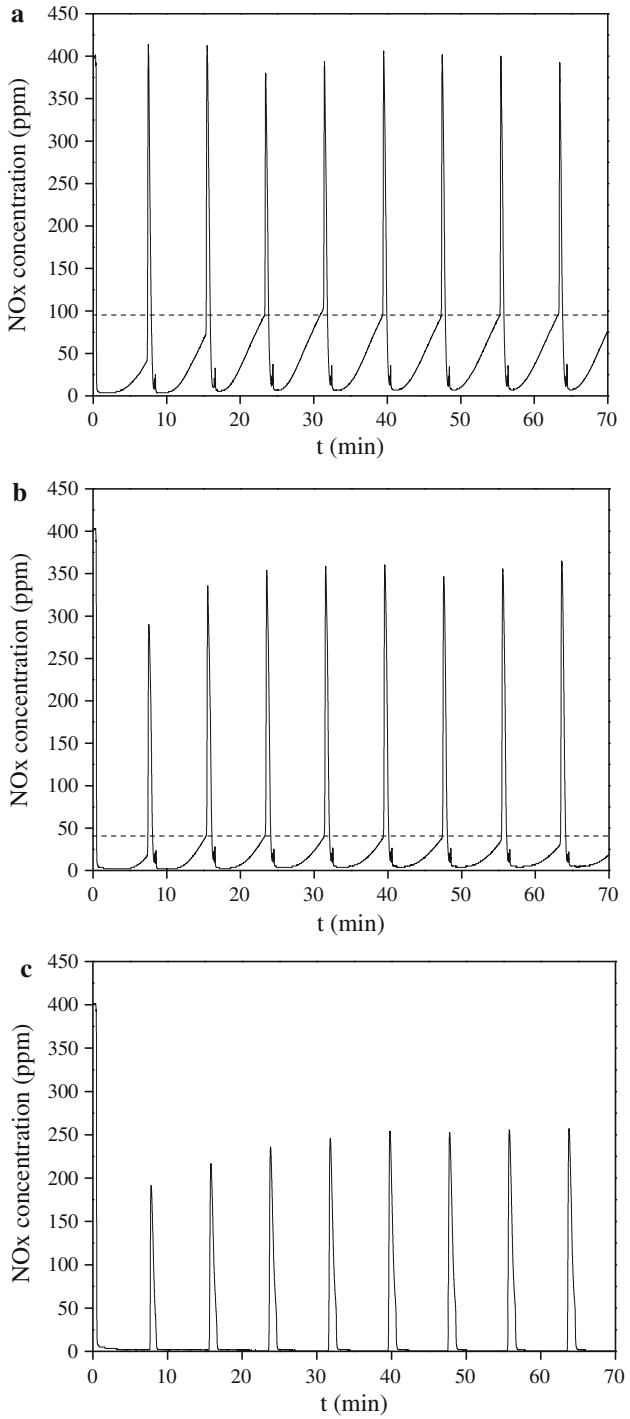

Fig. 7 Evolutions of NOx concentrations at lean-rich cycling condition over the catalysts prepared by different methods **a** Pt/K/TA-CO; **b** Pt/K/TA-CTAB; **c** Pt/K/TA-CTAB-OP

3.5 HR-TEM Analysis

To observe the dispersion state of platinum phase in nanoscale, high resolution TEM images of different catalysts were taken, as shown in Fig. 8. It is found that the Pt

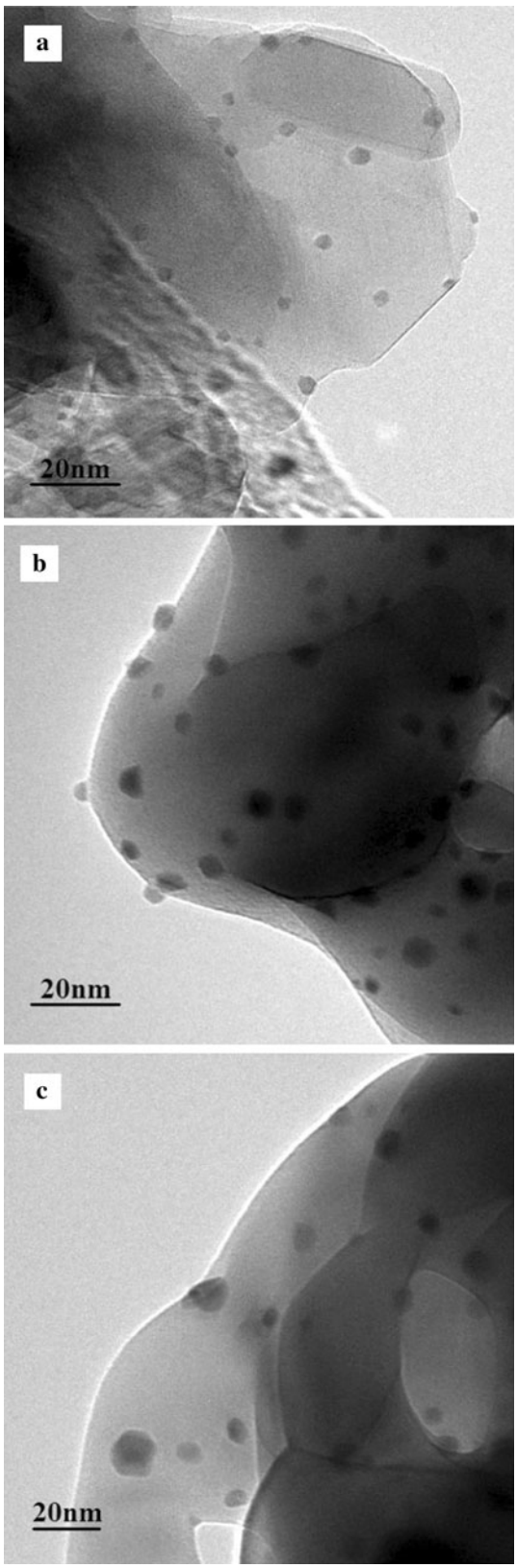

Fig. 8 HR-TEM images of the catalysts prepared by different methods **a** Pt/K/TA-CTAB-OP; **b** Pt/K/TA-CTAB; **c** Pt/K/TA-CO

particles in the catalyst Pt/K/TA-CTAB-OP are better dispersed, showing smaller average particle size (3.4 nm) as compared with that in Pt/K/TA-CTAB (4.7 nm) or Pt/K/TA-CO (5.1 nm). This result is in good consistence with the order for the average Pt particle size determined from H_2-chemisorption and the specific surface area of the supports (see Table 1); however, there exists obvious difference between the results from TEM and H_2-chemisorption, which should be mainly resulted from the systematic error of these two kinds of methods. It is well known that Pt is the key component during NO storage and reduction; the highly dispersed Pt could enhance the oxidation of NO to NO_2 and the successive storage as nitrate/nitrite at lean condition, meanwhile, it could remarkably facilitate the reduction of NOx at rich condition [23, 25]. Therefore, it is natural that the catalyst Pt/K/TA-CTAB-OP with higher Pt dispersion exhibits much better NOx storage and reduction performance than Pt/K/TA-CTAB and Pt/K/TA-CO.

4 Conclusive Remarks

The mesoporous binary mixed oxide TiO_2–Al_2O_3 (TA-CTAB-OP) was successfully synthesized by using CTAB and OP as co-templates, which possesses uniform pore size distribution and much higher specific surface area as compared with those prepared by using single template CTAB or by conventional co-precipitation method. Among the NSR catalysts with the supports prepared by different methods, the catalyst Pt/K/TA-CTAB-OP exhibits best NOx storage and reduction performance, giving a high NSC of 407 μmol/g and a mean NOx reduction percentage about 95 %, which is mainly attributed to the highest dispersion of Pt and storage component in this catalyst. In addition, the larger amount of surface acidic sites in the support TA-CTAB-OP determines that the catalyst Pt/K/TA-CTAB-OP also shows much better sulfur-resistance performance, giving a recovery efficiency as high as 94 %. Considering all the aspects such as NSC, NOx reduction percentage and desulfation/regeneration performance, the NSR catalyst Pt/K/TA-CTAB-OP is the most promising one for real application.

Acknowledgments This work is financially supported by the National Natural Science Foundation of China (No. 21076146), the Specialized Research Fund for the Doctoral Program of Higher Education of China (No. 20090032110013) and the Program of New Century Excellent Talents in University of China (No. NCET–07–0599). The authors are also grateful to the financial support from the State Key Laboratory of Engines at Tianjin University (No. K2012-05).

References

1. Cremona A, Fornasari G, Livi M, Petrini G, Trifirò F, Vaccari A, Vogna E (2008) Catal Lett 125:386
2. Weibel M, Waldbüßer N, Wunsch R, Chatterjee D, Bandl-Konrad B, Krutzsch B (2009) Top Catal 52:1702
3. Bögner W, Krämer M, Krutzsch B, Pischinger S, Voigtländer D, Wenninger G, Wirbeleit F, Brogan MS, Brisley RJ, Webster DE (1995) Appl Catal B 7(1–2):153
4. Büchel R, Pratsinis SE, Baiker A (2012) Appl Catal B 113–114:160
5. Luo JY, AL-Harbi M, Pang M, Epling WS (2011) Appl Catal B 106:664
6. Happel M, Desikusumastuti A, Sobota M, Laurin M, Libuda J (2010) J Phys Chem C 114:4568
7. Liu ZQ, Anderson JA (2004) J Catal 228:243
8. Zou ZQ, Meng M, Zhou XY, Li XG, Zha YQ (2009) Catal Lett 128:475
9. He JJ, Meng M, Zou ZQ, He XX (2010) Catal Lett 136:234
10. Hirata H, Hachisuka I, Ikeda Y, Tsuji S, Matsumoto S (2001) Top Catal 16/17:145
11. Zhao DY, Feng JL, Huo QS, Melosh N, Fredrickson GH, Chmelka BF, Stucky GD (1998) Science 279:548
12. Chaudhari K, Bal R, Chandwadkar AJ, Sivasanker S (2002) J Mol Catal A 177:247
13. Zou ZQ, Meng M, Luo JY, Zha YQ, Xie YN, Hu TD, Liu T (2006) J Mol Catal A 249:240
14. Song MG, Kim JY, Cho SH, Kim JD (2002) Langmuir 18:6110
15. Prinetto F, Manzoli M, Morandi S, Frola F, Ghiotti G, Castoldi L, Lietti L, Forzatti P (2010) J Phys Chem C 114:1127
16. Liu ZQ, Epling WS, Anderson JA (2011) J Phys Chem C 115:952
17. He XX, Meng M, He JJ, Zou ZQ, Li XG, Li ZQ, Jiang Z (2010) Catal Commun 12:165
18. Zou ZQ, Meng M, He JJ (2010) Mater Chem Phys 124:987
19. Feng X, Jiang GY, Zhao Z, Wang L, Li XH, Duan AJ, Liu J, Xu CM, Gao JS (2010) Energy Fuel 24:4111
20. Liu Y, Meng M, Li XG, Guo LH, Zha YQ (2008) Chem Eng Res Des 86:932
21. Kabin KS, Muncrief RL, Harold MP (2004) Catal Today 96:79
22. Pieta IS, García-Diéguez M, Herrera C, Larrubia MA, Alemany LJ (2010) J Catal 270:256
23. Wang XY, Yu YB, He H (2011) Appl Catal B 104:151
24. Arena GE, Bianchini A, Centi G, Vazzana F (2001) Top Catal 16/17:157
25. Castoldi L, Lietti L, Bonzi R, Artioli N, Forzatti P, Morandi S, Ghiotti G (2011) J Phys Chem C 115:1277